[3] J. O. Bergman and C. Christensen, "Equivalent circuit for a lumped element Y circulator," *IEEE Trans. Microwave Theory Tech.*, vol. MTT-16, pp. 308–310, May 1968.
[4] G. Bittar and Gy. Veszely, "A general equivalent network of the input impedance of symmetric three-port circulators," *IEEE Trans. Microwave Theory Tech.*, vol. MTT-28, pp. 807–808, July 1980.

# First-Order Bragg Interactions in a Gyromagnetic-Dielectric Waveguide

MAKOTO TSUTSUMI, MEMBER, IEEE

*Abstract*—**First-order Bragg interactions in a gyromagnetic-dielectric waveguide are investigated theoretically. With the aid of a singular perturbation procedure the coupled mode equations governing the nature of transverse electric wave interactions are derived. Bragg reflection characteristics are shown numerically as a function of the magnetic field.**

## I. Introduction

Bragg interaction in a planer dielectric waveguide whose properties vary periodically is very interesting topic from both practical and theoretical points of view [1]. Recently Seshadri has investigated asymmetric first-order Bragg interactions in a active dielectric waveguide by a singular perturbation procedure using multiple space scales [2]. The author has also studied the reflection of millimeter wave by a corrugated dielectric slab using a singular boundary procedure, and has confirmed the theoretical results by experiments [3].

This short paper investigates Bragg reflection characteristics in a gyromagnetic-dielectric waveguide whose refractive indexes vary sinusoidally in the direction of the wave propagation. Reflection characteristics in such a waveguide will be more sensitive to the change of the magnetic field than that of a corrugated gyromagnetic slab [4]. With the aid of a singular perturbation procedure using multiple scales the coupled mode equations are derived, and Bragg reflection characteristics as a function of the magnetic field are shown numerically.

## II. Analysis by a Singular Perturbation Procedure

A cross-sectional view of the gyometrical configuration and the system of coordinate used for the analysis are shown in Fig. 1(a). The permeability and permittivity of the slab have a sinusoidal variation in the $y$ direction, a surface of the slab is grounded by a metal plate, and the biasing magnetic field $H_i$ is applied to the $z$ direction. Such a slab structure can be realized by arranging a ferrite slab and a dielectric slab alternatively, and some chemical resins may be used for bonding these slabs, as shown in Fig. 1(b).

In millimeter-wave frequency the permeability tensor of the ferrite medium will be nearly equal to unity. At frequency 50 GHz with the magnetic field 5 Kg the diagonal and nondiagonal components of the ferrite medium (YIG) are 1.03 and 0.1,

Manuscript received October 8, 1980; revised April 10, 1981.
M. Tsutsumi is with the Faculty of Engineering, Osaka University, Suita 565, Japan.

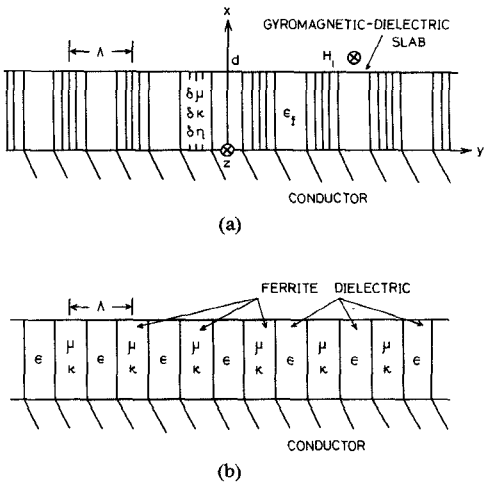


Fig. 1 System of coordinate used for analysis and structure of the periodic gyromagnetic-dielectric waveguide.

respectively [5]. Under this approximation the sinusoidal variation of the permeability tensor is assumed as

$$\hat{\mu}(y)=\mu_0\begin{bmatrix}1+\delta\mu & -j\delta\kappa & 0\\ j\delta\kappa & 1+\delta\mu & 0\\ 0 & 0 & 1\end{bmatrix} \tag{1}$$

where

$$\delta\mu=\delta\bar{\mu}\cos Ky$$
$$\delta\kappa=\delta\bar{\kappa}\cos Ky$$
$$\bar{\mu}=\frac{(\gamma\mu_0)^2MH_i}{(\gamma\mu_0H_i)^2-\omega^2}$$
$$\bar{\kappa}=\frac{\mu_0\gamma M\omega}{(\gamma\mu_0H_i)^2-\omega^2}$$

and $K=2\pi/\Lambda$.

$\delta$ represents a formal expansion parameter [2], [6], and [7] and $\Lambda$ is the periodicity of the sinusoidal variation of the permeability. The sinusoidal variation of the permittivity is also assumed as

$$\epsilon=\epsilon_f(1+\delta\eta\cos Ky). \tag{2}$$

In the above equations it is assumed that $\delta\bar{\mu}$, $\delta\bar{\kappa}$, and $\delta\eta$ are so small that only the first-order effect of the sinusoidal variation of the refractive indexes will be taken account.

We assume that the waves do not vary in the direction of the bias field ($\partial/\partial z=0$) and that they vary sinusoidally with time and angular frequency $\omega$, ($\exp(-j\omega t)$). The perturbed electric fields due to a sinusoidal variation of indexes can be expressed as

$$E_z=E_{z_0}(x,y_0,y_1)+\delta E_{z_1}(x,y_0,y_1)$$
$$\bar{E}_z=\bar{E}_{z_0}(x,y_0,y_1)+\delta\bar{E}_{z_1}(x,y_0,y_1) \tag{3}$$

where $E_{z_0}$ and $\bar{E}_{z_0}$ are the unperturbed zero-order fields in the slab and the vacuum, respectively, $E_{z_1}$ and $\bar{E}_{z_1}$ are the first-order correction terms due to the slight perturbation, and they are function of $y_0=y$ and $y_1=\delta y$ [6]. The angular frequency $\omega$ in the vicinity of the Bragg frequency $\omega_0$ can be expanded as

$$\omega=\omega_0+\delta\omega_1. \tag{4}$$

The chain rule of the differentiation yields [6]

$$\partial/\partial y=\partial/\partial y_0+\delta\partial/\partial y_1. \tag{5}$$

0018-9480/81/1000-1111$00.75 ©1981 IEEE

Substituting (1)–(5) into Maxwell's equations and equating the coefficients of equal powers of $\delta$ on both sides, the following Helmholtz equations can be obtained:

$$\partial^2 E_{z_0}/\partial x^2+\partial^2 E_{z_0}/\partial y_0^2+\omega_0^2\mu_0\epsilon_f E_{z_0}=0 \tag{6}$$

$$\begin{aligned}\partial^2 E_{z_1}/\partial x^2+\partial^2 E_{z_1}/\partial y_0^2+\omega_0^2\mu_0\epsilon_f E_{z_1}&\\ =-\{2\partial^2 E_{z_0}/\partial y_0\partial y_1+\bar{\mu}\omega_0^2\mu_0\epsilon_f E_{z_0}\cos Ky&\\ +K\sin Ky(\bar{\mu}\partial E_{z_0}/\partial y_0+j\bar{\kappa}\partial E_{z_0}/\partial x)&\\ +\omega_0\mu_0\epsilon_f(\omega_0\eta\cos Ky+2\omega_1)E_{z_0}\}.&\end{aligned} \tag{7}$$

Helmholtz equations in the vacuum region can be obtained from (6) with $E_{z_0}=\bar{E}_{z_0}$, $\epsilon_f=\epsilon_0$ and (7) with $E_{z_0}=\bar{E}_{z_0}$, $E_{z_1}=\bar{E}_{z_1}$, $\epsilon_f=\epsilon_0$, and $\bar{\mu}=\bar{\kappa}=\eta=0$.

The zero-order field solution of (6) satisfying the boundary condition at infinity ($x=+\infty$) can be assumed to have the superposition of the forward and backward waves:

$$\bar{E}_{z_0}=C_0^+\sin k_x^+ d\cdot e^{\gamma^+(d-x)}e^{j\beta^+ y_0}+C_0^-\sin k_x^- d\cdot e^{\gamma^-(d-x)}e^{-j\beta^- y_0}$$

$$E_{z_0}=C_0^+\sin k_x^+ x\cdot e^{j\beta^+ y_0}+C_0^-\sin k_x^- x\cdot e^{-j\beta^- y_0} \tag{8}$$

where

$$k_x^\pm=\sqrt{\omega_0^2\mu_0\epsilon_f-(\beta^\pm)^2}$$

$$\gamma^\pm=\sqrt{(\beta^\pm)^2-\omega_0^2\mu_0\epsilon_0}.$$

In the above expressions, the superscript + and − on the wave amplitude $C_0$ and the propagation constant $\beta$ indicate the forward and the backward waves, respectively.

On a slab whose boundary surface is open to vacuum, the tangential component of the electric field $E_{z_0}$, ($E_{z_1}$) and the magnetic field $H_{y_0}$, ($H_{y_1}$) must be continuous across the boundary surface of $x=d$. Also the tangential component of the electric field must vanish at the metal boundary of $x=0$; $E_{z_0}$, $E_{z_1}=0$.

Substituting (8) into boundary conditions, we get the zero-order dispersion relation of TE waves in dielectric image line [8]:

$$\tan k_x^\pm d=-\frac{k_x^\pm}{\gamma^\pm}. \tag{9}$$

In general the $n$th harmonic wave propagating through a periodic structure couples primarily to the $(n-1)$th harmonic and indirectly to others. Thus the coupling to the higher harmonics is neglected, and attention is concentrated on the vicinity of the symmetric Bragg coupling region where $n=0$ and $n=-1$ space harmonics intersect each other. The relation between the propagation constant $\beta^+$ and $\beta^-$ of $n=0$ and $n=-1$ modes, respectively, at the interaction point, is given by

$$\beta^+=\beta^-=\beta=K/2. \tag{10}$$

The first-order perturbed fields $E_{z_1}$ and $\bar{E}_{z_1}$ are assumed to be in the form

$$\begin{aligned}\bar{E}_{z_1}&=g^+(x)e^{j\beta y_0}+g^-(x)e^{-j\beta y_0}\\ E_{z_1}&=f^+(x)e^{j\beta y_0}+f^-(x)e^{-j\beta y_0}.\end{aligned} \tag{11}$$

Substituting (8) and (11) into the first-order Helmholz equation (7) and using the orthogonality relations of the Floquet modes $\exp(j\beta^+ y)$ and $\exp(-j\beta^- y)$ with the help of (10), we obtain the solutions of the first-order Helmholz equation. Substituting (8) and (11) into boundary conditions satisfied by $E_{z_1}$ and $H_{y_1}$, and with the help of (10), $g(x)$ and $f(x)$ at $x=d$, the boundary conditions for the first order are expressed in term of $\exp(\mp j\beta y)$:

$$\begin{aligned}F_1-\sin k_x d\cdot C_1&=P_1^\pm\\ \gamma F_1+\cos k_x d\cdot k_x C_1&=P_2^\pm\end{aligned} \tag{12}$$

where

$$\begin{aligned}p_1^\pm=&\frac{d\sin k_x d}{\gamma}\left\{\mp j\beta\frac{\partial C_0^\pm}{\partial y_1}-\omega_1\omega_0\mu_0\epsilon_0 C_0^\pm\right\}\\ &+\frac{d\cos k_x d}{k_x}\left\{\pm j\beta\frac{\partial C_0^\pm}{\partial y_1}+\omega_1\omega_0\mu_0\epsilon_f C_0^\pm\right\}\\ &+\frac{d\cos k_x d}{4k_x}\left\{\omega_0^2\mu_0\epsilon_f\eta-\bar{\mu}\left(K\beta-\omega_0^2\mu_0\epsilon_f\right)\right\}C_0^\mp\\ &\mp\frac{K\bar{\kappa}}{4}d\sin K_x d\cdot C_0^\mp\\ p_2^\pm=&\frac{\sin k_x d}{\gamma}\left\{\pm j\beta\frac{\partial C_0^\pm}{\partial y_1}+\omega_1\omega_0\mu_0\epsilon_0 C_0^\pm\right\}(1-\gamma d)\\ &+\gamma\frac{\omega_1}{\omega_0}\sin k_x d\cdot C_0^\pm\\ &+\frac{1}{k_x}(\cos k_x d-k_x d\sin k_x d)\\ &\cdot\left\{\mp j\beta\frac{\partial C_0^\pm}{\partial_{y_1}}-\omega_1\omega_0\mu_0\epsilon_f C_0^\pm-\frac{\omega_0^2}{4}\mu_0\epsilon_f\eta C_0^\mp\right.\\ &\left.+\frac{\bar{\mu}}{4}C_0^\mp\left(K\beta-\omega_0^2\mu_0\epsilon_f\right)\right\}\\ &+\left(\frac{\omega_1}{\omega_0}k_x C_0^\pm+\frac{\bar{\mu}}{2}k_x C_0^\mp\right)\\ &\cdot\cos k_x d+\frac{\bar{\kappa}\beta}{2}\sin K_x d\cdot C_0^\mp\\ &\pm\frac{K}{4}\bar{\kappa}(\sin k_x d+dk_x\cos k_x d)C_0^\mp.\end{aligned}$$

Eliminating constants $F_1$ and $C_1$ in (12) by using the zero-order dispersion relation (9), we get the coupled mode equations for the Floquet modes $\exp(j\beta y)$ and $\exp(-j\beta y)$ as

$$\begin{aligned}\omega_1 C_0^+ +jv_g\frac{\partial C_0^+}{\partial y_1}&=cC_0^-\\ \omega_1 C_0^- -jv_g\frac{\partial C_0^-}{\partial y_1}&=cC_0^+\end{aligned} \tag{13}$$

where

$$c=-\frac{\left[\frac{\gamma}{k_x^2}(1+\gamma d)+d\right]\left[\eta\omega_0^2\mu_0\epsilon_f-\bar{\mu}\left(K\beta-\omega_0^2\mu_0\epsilon_f\right)\right]-2\bar{\mu}\gamma}{4\omega_0\mu_0\left\{\epsilon_f\left[\left(1+\frac{\gamma^2}{k_x^2}\right)d+\frac{\gamma}{k_x^2}\right]+\frac{\epsilon_0}{\gamma}\right\}}.$$

In the above equations $v_g$ is the group velocity obtained by differentiating (9) with respect to $\omega_0$. In the limiting case where the $\eta$ becomes zero in (13), the coupling coefficient is only a function of $\bar{\mu}$. In this condition Bragg reflection characteristics will be very sensitive to the change of the magnetic field.

## III. Numerical Examples and Discussions

If the waves having amplitude $C_0$ in (13) have the form of $C_{00}\exp(j\beta_1 y)$, the first-order dispersion relation in the vicinity of the symmetric Bragg interaction can be obtained [2]. The typical

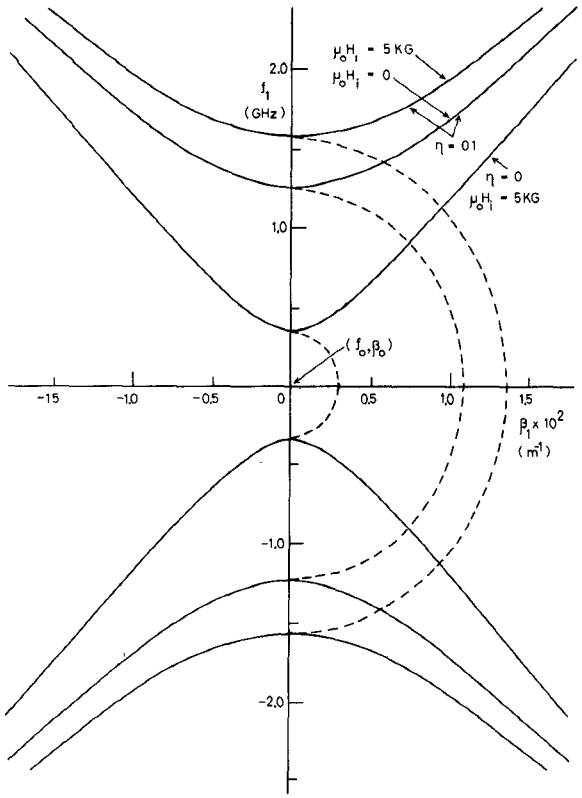


Fig. 2 Symmetric first-order stopband characteristics as a function of the modulation index and the magnetic field.

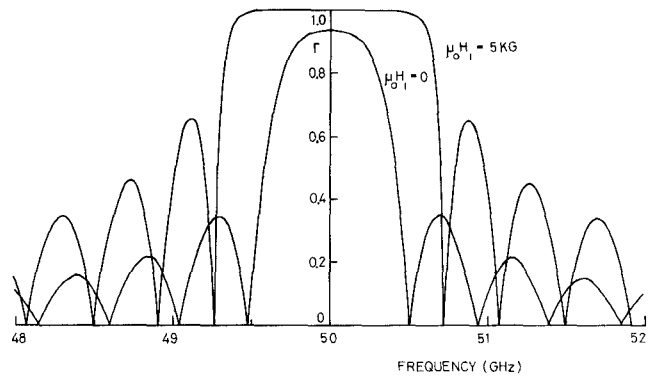


Fig. 3 Bragg reflection characteristics as a function of the magnetic field.

Brillouin diagram calculated from the first-order dispersion relation is presented in Fig. 2 for various values of the modulation index of the permittivity and the magnetic field. In this figure, Bragg interaction point $(f_0, \beta_0)$ is estimated from the zero-order dispersion relation (9) of the fundamental mode of TE waves. The material constant used for numerical computations are $\epsilon_f/\epsilon_0 = 15.7$, $d=2.0$ mm, $\mu_0 M = 1890$ G, $\gamma = 1.76 \times 10^{11}$ $(\text{Wb/m}^2\text{s})^{-1}$ and $\Lambda = 0.794$ mm, where the periodicity $\Lambda$ is given by $\Lambda = \pi/\beta_0$, ($\beta_0 = 3.957 \times 10^3$ $\text{m}^{-1}$ for $f_0 = \omega_0/(2\pi) = 50$ GHz). It can be seen from Fig. 2 that the stop bandwidth of the range from 2.5 to 3.2 GHz for $\eta = 0.1$ changes if the magnetic field is varied from zero to 5 kG, as also the complex value of the propagation constant as shown by dashed lines.

The present theory is based on the assumption that the sinusoidally modulated refractive index is of infinite length. If the end effects are negligible, we can apply this theory to the modulated refractive index of infinite length.

Let us assume that a TE wave is incident on the modulated refractive index region at $y=0$ and that a wave is partly transmitted through the modulated refractive index region at $y=D$. The reflection coefficient $\Gamma$ can be derived from the solution of the boundary conditions at propagation direction [7]. The reflection coefficient is estimated numerically as a function of the frequency and the magnetic field. The result is shown in Fig. 3. The material parameters used for calculation are the number of the modulated index $N=100$, $\eta=0.02$, and $d=2.0$ mm. It is interesting to note that the stop bandwidth of about 1.2 GHz of the reflection (filter) characteristics and the return loss can be controlled by the dc magnetic field, and their characteristics have not been found for the corrugated gyromagnetic slab [4].

The coupling mode equations for asymmetric Bragg interaction can be derived in the same way as that for symmetric interaction

[2]. But we have found that the asymmetric interaction is not sensitive to the change of the magnetic field.

## IV. Conclusion

First-order Bragg interaction in a gyromagnetic-dielectric waveguide is analyzed by a singular perturbation procedure. The expression for the dispersion relation in the vicinity of the Bragg frequency is derived. The Bragg reflection characteristics are shown numerically. It is found that the stop bandwidth and maximum decay of waves due to Bragg interaction can be controlled by the magnetic field.

The result given in the present paper may be useful designing millimeter-wave devices such as tunable filters and electrically scannable leaky wave antenna [9].

## Acknowledgment

The author would like to thank Prof. Nobuaki Kumagai of Osaka University for his valuable discussions and encouragement.

## References

[1] C. Elachi, "Waves in active and passive periodic structures: A review," *Proc. IEEE.*, vol. 64, pp. 1666–1698, Dec. 1976.
[2] S. R. Seshadri, "Asymmetric first-order Bragg interactions in an active dielectric waveguide," *Appl. Phys.*, vol. 17, pp. 141–149, 1978.
[3] M. Tsutsumi, T. Ohira, T. Yamaguchi, and N. Kumagai, "Reflection of millimeter waves by a corrugated dielectric slab waveguide," *Proc. IEEE*, vol. 68, pp. 733–734, June 1980.
[4] M. Tsutsumi and N. Kumagai, "Reflection of millimeter waves by a corrugated ferrite slab," *Proc. IEEE*, vol. 69, pp. 1083–1084, Aug. 1981.
[5] Lax and Button, "Microwave ferrite and ferrimagnetics," New York: McGraw-Hill, 1962.
[6] S. R. Seshadri, Asymptotic theory of mode coupling in a space-time periodic medium-part 1: stable interactions," *Proc. IEEE.*, vol. 65, pp. 996–1004, July 1977.
[7] S. R. Seshadri, "Love wave interaction in a thin film with a periodic surface corrugation," *IEEE. Trans. Sonics Ultrason.*, vol. SU-25, 6, pp. 378–383, Nov. 1978.
[8] R. F. Harrington, *Time-Harmonic Electromagnetic Fields* New York: McGraw-Hill, 1961.
[9] R. E. Horn, H. Jacobs, E. Freibergs, and K. Klohn, "Electronic modulated beam steerable silicon waveguide array antenna," *IEEE. Trans. Microwave Theory Tech.*, vol. MTT-28, pp. 647–653, June 1980.

# Microwave Pulse-Induced Acoustic Resonances in Spherical Head Models

RICHARD G. OLSEN AND JAMES C. LIN, SENIOR MEMBER, IEEE

*Abstract*— **Microwave-induced acoustic pressures in spherical models of human and animal heads are measured using a small hydrophone transducer. The measured acoustic frequencies that correspond to mechanical resonance of the head model agree with those predicted by the thermoelastic theory of interaction. Further, a three-pulse burst applied at appropriate pulse repetition frequencies could effectively drive the model to respond in such a manner that the microwave-induced pressure amplitude would increase by threefold or more.**

Manuscript received February 2, 1981; revised April 30, 1981. This work was supported in part by the U. S. Navy Medical Research and Development Command and in part by the National Science Foundation

R. G. Olsen is with the Naval Aerospace Medical Research Laboratory, Pensacola, FL 32508.

J. C. Lin is with the Bioengineering Program, University of Illinois at Chicago Circle, Chicago, IL 60680.

## I. Introduction

Auditory responses are evoked in human beings and laboratory animals irradiated with rectangular-pulse, modulated microwave energy [1]–[3]. Most investigators of this phenomena believe that the response stems from microwave-induced thermoelastic expansion [4]–[8], i.e., when microwave radiation impinges on the head, a portion of the absorbed energy is converted into heat which produces a miniscule but rapid rise of temperature in the tissues of the head. This rise of temperature ($\sim 10^{-6}$ °C) occurring in a very short time (10 $\mu$s) generates rapid thermoelastic expansion of the brain matter or other tissues in the head which then launches an acoustic wave of pressure that is detected by the hair cells in the cochlea [9].

This thermoelastic theory which covers many experimental observations [8]–[10], suggests among other characteristics that the frequency of the auditory signal is a function of the size and acoustic property of tissues in the head [11]–[12]. Specifically, the fundamental frequency of sound was found to be given by

$$f_s = 3.14\nu/(3\pi a) \tag{1}$$

for stress-free surfaces [11]. Thus, the microwave-induced sound is a function of sound propagation speed ($\nu$), and the radius ($a$) or circumference ($2\pi a$) of the head. To date, experimental support for this observation comes primarily from measured cochlear microphonics in cats and guinea pigs [10], [13], [14], and the well-documented requirement for human preception of pulsed microwaves; i.e., the ability to hear high-frequency sound [1]–[3]. However, direct experimental confirmation for the mechanical resonances inside the head has yet to appear in the literature. This paper presents direct hydrophone measures of pulsed microwave-induced acoustic signals in variously sized spherical head models filled with brain-equivalent materials.

## II. Methods and Materials

### A. Models

The spherical models were composed of hemispherical voids carefully machined in 20.3×20.3×7.6-cm blocks of foamed polystyrene and filled with brain-equivalent materials. The foamed polystyrene provided a stress-free boundary to the brain model. The electromagnetic, mechanical, and thermal properties of the brain-equivalent material are similar to brain tissues. It is made from gelling agent, finely granulated polyethylene powder, sodium chloride and water [15]. It has a sonic propagation speed of 1600 m/s at room temperature [16]. Typically, two-kilogram batches of the brain-equivalent material were prepared and then evacuated for approximately 30 min to remove included air.

### B. Hydrophone Transducer

A spherical hydrophone, 1 cm in diameter, was used in all experiments (Edo Western Inc., Model 6600). The barium titanate piezoelectric element had a response of 50.1 pA/mV for the range of frequencies encountered in this study. The hydrophone was placed in the center of the model. Its output signal was displayed on an oscilloscope and photographed on Polaroid film.

### C. Microwave Irradiation Procedure

Pulsed microwave energy at 1.10 GHz and 4-kW peak power was obtained from an Epsco PG5KB generator. The microwave

0018-9480/81/1000-1114$00.75 ©1981 IEEE